

## Preparation and HREM Characterization of a Protonated Form of a Layered Perovskite Tantalate from an Aurivillius Phase $\text{Bi}_2\text{SrTa}_2\text{O}_9$ via Acid Treatment

Yu Tsunoda,<sup>†</sup> Masashi Shirata,<sup>†</sup> Wataru Sugimoto,<sup>‡</sup> Zheng Liu,<sup>§</sup> Osamu Terasaki,<sup>§,||</sup> Kazuyuki Kuroda,<sup>†,⊥</sup> and Yoshiyuki Sugahara<sup>\*,†</sup>

Department of Applied Chemistry, School of Science and Engineering, Waseda University, Shinjuku-ku, Tokyo 169-8555, Japan, Department of Fine Materials Engineering, Faculty of Textile Science and Technology, Shinshu University, Ueda, Nagano 386-8567, Japan, CREST, JST, Tohoku University, Aoba-ku, Sendai, Miyagi 980-8578, Japan, Department of Physics, Graduate School of Science and CIR, Tohoku University, Aoba-ku, Sendai, Miyagi 980-8578, Japan, and Kagami Memorial Laboratory for Materials Science and Technology, Waseda University, Nishiwaseda-2, Shinjuku-ku, Tokyo 169-0051, Japan

Received March 9, 2001

An Aurivillius phase,  $\text{Bi}_2\text{SrTa}_2\text{O}_9$ , which consists of perovskite-like slabs and bismuth oxide sheets, was treated with 3 M hydrochloric acid for 72 h, and the resultant product was characterized. Scanning electron microscopy investigation indicated that no morphological change occurred during the acid treatment. X-ray diffraction (XRD) analysis revealed that the product exhibited tetragonal symmetry with  $a = 0.391 \pm 0.004$  nm and  $c = 0.98 \pm 0.01$  nm, and the  $a$  parameter is consistent with a typical value for cubic perovskite oxides. High-resolution electron microscopy (HREM) observations along both [001] and [010] showed that the structure of the perovskite-like slabs in  $\text{Bi}_2\text{SrTa}_2\text{O}_9$  was retained after the acid treatment. The compositional analyses revealed the loss of a large portion of bismuth and a part of strontium (present in the bismuth oxide sheets due to  $\text{B} \leftrightarrow \text{Sr}$  disorder) and the introduction of protons. These observations indicate that the bismuth oxide sheets in  $\text{Bi}_2\text{SrTa}_2\text{O}_9$  were selectively leached and that protons were introduced into the interlayer space to form a protonated layered perovskite,  $\text{H}_{1.8}[\text{Sr}_{0.8}\text{Bi}_{0.2}\text{Ta}_2\text{O}_7]$ . Though diffraction techniques (XRD and electron diffraction) demonstrated that an average structure of  $\text{H}_{1.8}[\text{Sr}_{0.8}\text{Bi}_{0.2}\text{Ta}_2\text{O}_7]$  consisted of perovskite-like slabs stacked without displacement, HREM observation along [010] demonstrated that both a simple stacking sequence without displacement ( $P$ -type) and a stacking sequence with a relative displacement by  $(a + b)/2$  ( $I$ -type) were present in  $\text{H}_{1.8}[\text{Sr}_{0.8}\text{Bi}_{0.2}\text{Ta}_2\text{O}_7]$ .

### Introduction

Ion-exchangeable, layered perovskites consist of negatively charged perovskite-like slabs and interlayer monovalent cations, and two series of oxides are known: Dion–Jacobson phases,  $\text{M}[\text{A}_{n-1}\text{B}_n\text{O}_{3n+1}]$ ,<sup>1,2</sup> and Ruddlesden–Popper phases,  $\text{M}_2[\text{A}_{n-1}\text{B}_n\text{O}_{3n+1}]$  ( $\text{M} = \text{Rb}, \text{K}, \text{etc.}; \text{A} = \text{Sr}, \text{Ca}, \text{La}, \text{etc.}; \text{B} = \text{Ti}, \text{Nb}, \text{and Ta}; \text{and } n = \text{perovskite-like slab thickness}$ ).<sup>3,4</sup> Aurivillius phases (expressed as  $\text{Bi}_2\text{A}_{n-1}\text{B}_n\text{O}_{3n+3}$  or  $\text{Bi}_2\text{O}_2\text{[A}_{n-1}\text{B}_n\text{O}_{3n+1}]$ ), whose ferroelectric properties have attracted attention, also possess perovskite-like slabs; their structures can be considered to be intergrowths of perovskite-like slabs and bismuth oxide sheets.<sup>5</sup>

Protonated forms of layered perovskites ( $\text{H}_x[\text{A}_{n-1}\text{B}_n\text{O}_{3n+1}]$ ,  $x = 1$  or 2) are generally obtained via acid treatments of ion-

exchangeable, layered perovskites through exchange reactions of interlayer cations with protons.<sup>2,4,6–9</sup> We have reported that the acid treatment of an Aurivillius phase,  $\text{Bi}_2\text{SrNaNb}_3\text{O}_{12}$ , resulted in the formation of a protonated form of a layered perovskite by the selective leaching of the bismuth oxide sheets and the corresponding introduction of protons for charge compensation.<sup>10</sup> Thus, the overall reaction was the substitution of the bismuth oxide sheets with protons without changing the perovskite-like slab structure. Although the B-site cations of the ion-exchangeable, layered perovskites are limited to Ti, Nb, and Ta,<sup>11</sup> various metal cations such as Fe, Mn, Ti, Nb, Ta, W, and Mo can be present at the B-sites of the Aurivillius phases.<sup>12</sup> Consequently, a variety of protonated forms of layered perovskites could be derived from the Aurivillius phases.

<sup>†</sup> School of Science and Engineering, Waseda University.

<sup>‡</sup> Shinshu University.

<sup>§</sup> CREST, JST, Tohoku University.

<sup>||</sup> Graduate School of Science and CIR, Tohoku University.

<sup>⊥</sup> Kagami Memorial Laboratory for Materials Science and Technology, Waseda University.

- (1) Dion, M.; Ganne, M.; Tournoux, M. *Mater. Res. Bull.* **1981**, *16*, 1429.
- (2) Jacobson, A. J.; Johnson, J. W.; Lewandowski, J. T. *Inorg. Chem.* **1985**, *24*, 3727.
- (3) (a) Ruddlesden, S. N.; Popper, P. *Acta Crystallogr.* **1957**, *10*, 538. (b) Ruddlesden, S. N.; Popper, P. *Acta Crystallogr.* **1958**, *11*, 54.
- (4) Gopalakrishnan, J.; Bhat, V. *Inorg. Chem.* **1987**, *26*, 4299.
- (5) (a) Aurivillius, B. *Ark. Kemi* **1949**, *1*, 463. (b) Aurivillius, B. *Ark. Kemi* **1950**, *2*, 519. (c) Aurivillius, B. *Ark. Kemi* **1952**, *5*, 39. (d) Frit, B.; Mercurio, J. P. *J. Alloys Compd.* **1992**, *188*, 27.

- (6) Jacobson, A. J.; Lewandowski, J. T.; Johnson, J. W. *J. Less-Common Met.* **1986**, *116*, 137.
- (7) Dion, M.; Ganne, M.; Tournoux, M. *Rev. Chim. Miner.* **1986**, *23*, 61.
- (8) Ollivier, P. J.; Mallouk, T. E. *Chem. Mater.* **1998**, *10*, 2585.
- (9) (a) Bhuvanesh, N. S. P.; Crosnier-Lopez, M.-P.; Duroy, H.; Fourquet, J.-L. *J. Mater. Chem.* **2000**, *10*, 1685. (b) Crosnier-Lopez, M. P.; Le Berre, F.; Fourquet, J.-L. *J. Mater. Chem.* **2001**, *11*, 1146–1151.
- (10) Sugimoto, W.; Shirata, M.; Sugahara, Y.; Kuroda, K. *J. Am. Chem. Soc.* **1999**, *121*, 11601.
- (11) (a) Gopalakrishnan, J. *Rev. Solid State Sci.* **1988**, *1*, 515. (b) Toda, K.; Sato, M. *J. Mater. Chem.* **1996**, *6*, 1067.
- (12) (a) Rao, C. N. R.; Raveau, B. *Transition Metal Oxide*, 2nd ed.; Wiley-VCH: New York, 1998; pp 74–75. (b) Kubel, F.; Schmid, H. *Ferroelectrics* **1992**, *129*, 101. (c) Mahesh-kumar, M.; Srinivas, A.; Kumar, G. S.; Suryanarayana, S. V. *Solid State Commun.* **1997**, *104*, 741.

Here, we report the conversion of another Aurivillius phase,  $\text{Bi}_2\text{SrTa}_2\text{O}_9$ , into a protonated form of a layered perovskite via acid treatment. The acid treatment of single-crystal  $\text{Bi}_2\text{SrTa}_2\text{O}_9$  was previously reported,<sup>13</sup> but the variation in the XRD patterns was interpreted as a structural change of the perovskite-like slabs in  $\text{Bi}_2\text{SrTa}_2\text{O}_9$  during the acid treatment. In the present study,  $\text{Bi}_2\text{SrTa}_2\text{O}_9$  powder was treated with 3 M hydrochloric acid, and the resultant product was fully characterized. Furthermore, we discuss the structure of the acid-treated product on the basis of transmission electron microscopy observation.

### Experimental Section

**Preparation of  $\text{Bi}_2\text{SrTa}_2\text{O}_9$ .**  $\text{Bi}_2\text{SrTa}_2\text{O}_9$  was prepared from a stoichiometric mixture of  $\text{Bi}_2\text{O}_3$ ,  $\text{SrCO}_3$ , and  $\text{Ta}_2\text{O}_5$  by solid-state reactions. The heating schedule is based on the preparative method used for  $\text{Bi}_2\text{SrNb}_2\text{O}_9$ ; the starting compounds were thoroughly ground and heated at 900 °C for 15 h, 1000 °C for 15 h, and 1200 °C for 24 h with intermittent grinding.<sup>14</sup>

**Acid Treatment of  $\text{Bi}_2\text{SrTa}_2\text{O}_9$ .** About 1 g of  $\text{Bi}_2\text{SrTa}_2\text{O}_9$  was dispersed in 200 mL of 3 M hydrochloric acid for 72 h. The acid-treated product was centrifuged, washed with water, and air-dried. The air-dried product was further heated at 120 °C under ambient atmosphere.

**Analyses.** The amounts of metals were determined by inductively coupled plasma emission spectrometry (ICP; Nippon Jarrell Ash, ICAP575 MarkII) after the samples were dissolved by heating in a mixture of HCl,  $\text{HNO}_3$ , and HF at 200 °C for at least 2 h. The amount of hydrogen was determined by thermogravimetry (TG; MacScience, TG-DTA2000S, 10 °C/min). X-ray diffraction (XRD) patterns were obtained by using a Rigaku RINT-2500 diffractometer (monochromated Cu K $\alpha$  radiation). A Rietveld analysis of  $\text{Bi}_2\text{SrTa}_2\text{O}_9$  was performed by using the program RIETAN.<sup>15</sup> Lattice parameters of the acid-treated product were refined by the nonlinear least-squares method. Electron diffraction (ED) patterns and high-resolution electron microscopy (HREM) images were obtained using a transmission electron microscope (TEM; JEOL JEM-4000EX) operated at 400 kV. Morphology was studied by scanning electron microscopy (SEM; Hitachi S-5000).

### Results and Discussion

**Acid Treatment of  $\text{Bi}_2\text{SrTa}_2\text{O}_9$ .** Scanning electron micrographs of  $\text{Bi}_2\text{SrTa}_2\text{O}_9$  and its acid-treated product are shown in Figure 1. Both  $\text{Bi}_2\text{SrTa}_2\text{O}_9$  and the acid-treated product consist of particles with diameters of 1–5  $\mu\text{m}$ , and no notable change in particle shape is observed, indicating that the dissolution of  $\text{Bi}_2\text{SrTa}_2\text{O}_9$  and subsequent precipitation are very unlikely.

XRD patterns of  $\text{Bi}_2\text{SrTa}_2\text{O}_9$  and its acid-treated product are shown in Figure 2. The XRD pattern of  $\text{Bi}_2\text{SrTa}_2\text{O}_9$  (Figure 2a) can be indexed on the basis of an orthorhombic cell ( $a = 0.5520(4)$  nm,  $b = 0.5521(4)$  nm,  $c = 2.505(2)$  nm), consistent with a previous report ( $a = 0.5525(4)$  nm,  $b = 0.5526(6)$  nm,  $c = 2.508(5)$  nm; space group,  $A2_1am$ ).<sup>16</sup> The  $a$  and  $b$  parameters correspond to  $\sqrt{2}a_p$  ( $a_p$  is the lattice parameter of the cubic perovskite oxides and is ca. 0.39 nm). It is also noted that two perovskite-like slabs are present in the unit cell, which is shown by a doubled  $c$  parameter of  $\text{Bi}_2\text{SrTa}_2\text{O}_9$  ( $c/2 = 1.25$  nm). The crude acid-treated product showed broad peaks, which can be indexed on the basis of a tetragonal cell. After heating at 120 °C, we found that the XRD peaks became sharper, and the acid-

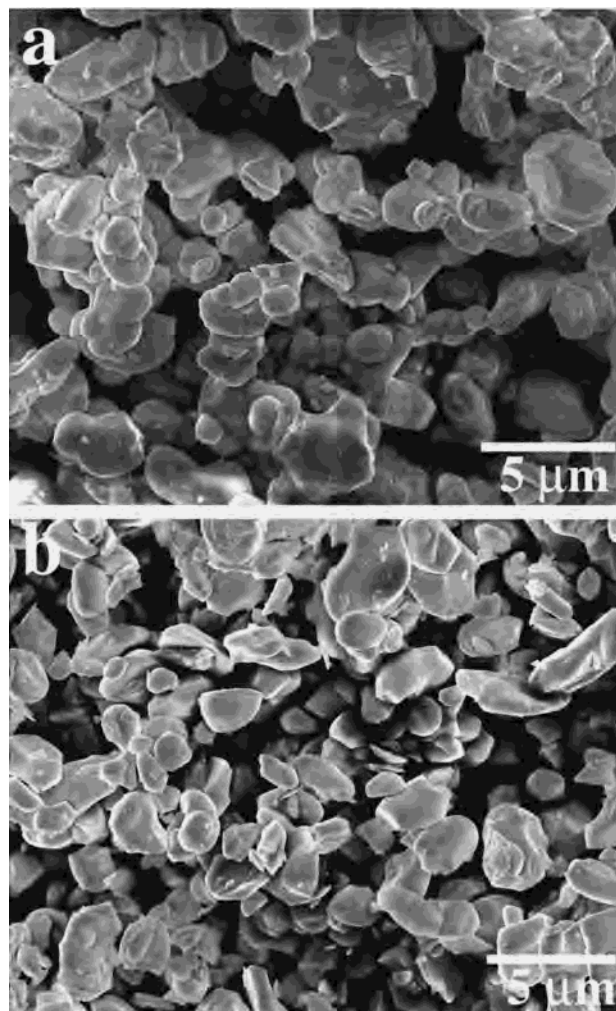


**Figure 1.** Scanning electron micrographs of (a)  $\text{Bi}_2\text{SrTa}_2\text{O}_9$  and (b) acid-treated  $\text{Bi}_2\text{SrTa}_2\text{O}_9$ .

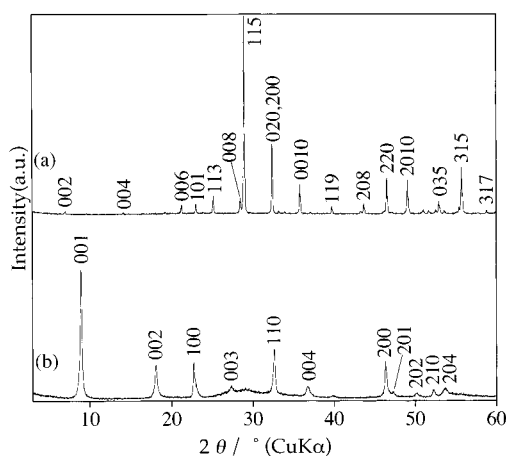


**Figure 2.** XRD patterns of (a)  $\text{Bi}_2\text{SrTa}_2\text{O}_9$  and (b) acid-treated  $\text{Bi}_2\text{SrTa}_2\text{O}_9$ .

treated product heated at 120 °C also exhibits tetragonal symmetry (Figure 2b). The lattice parameters of the acid-treated product heated at 120 °C are  $a = 0.391 \pm 0.004$  nm and  $c = 0.98 \pm 0.01$  nm. It should be noted that the lattice parameter  $a$  of the acid-treated product heated at 120 °C is in good agreement with the  $a_p$  value.

Figure 3a shows the ED pattern of the acid-treated product along the [001] zone and the corresponding HREM image of the acid-treated product. The ED pattern can be indexed on the

- (13) Suzuki, M.; Nagasawa, N.; Machida, A.; Ami, T. *Jpn. J. Appl. Phys.* **1996**, *35*, L564.  
 (14) Ismunandar; Kennedy, B. J.; Gunawan; Marsongkohadi *J. Solid State Chem.* **1996**, *126*, 135–141.  
 (15) (a) Izumi, F. In *Rietveld Analysis*; Young, R. A., Ed.; Oxford University Press: Oxford, 1993; pp 236–253. (b) Kim, Y. I.; Izumi, F. *J. Ceram. Soc. Jpn.* **1994**, *102*, 401.  
 (16) Rae, A. D.; Thompson, J. G.; Withers, R. L. *Acta Crystallogr.* **1992**, *B48*, 418.

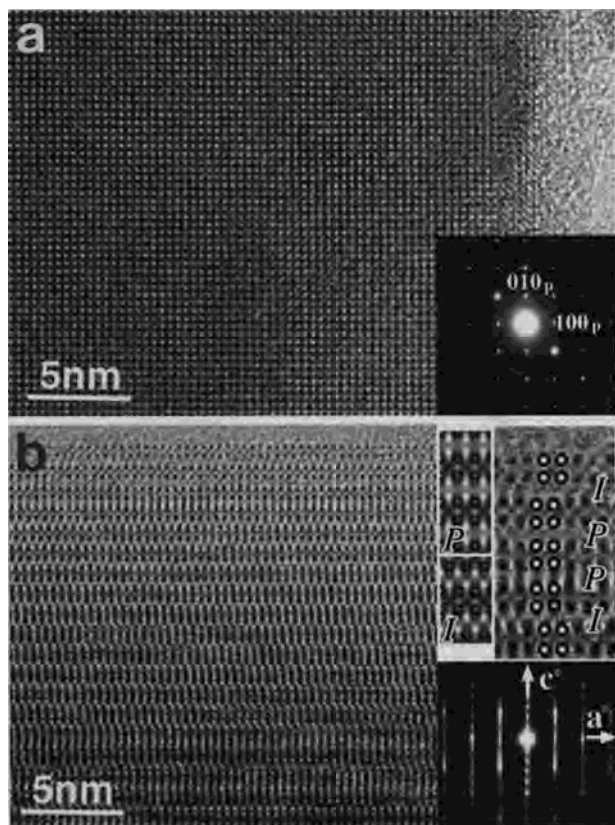


**Figure 3.** HREM images of acid-treated  $\text{Bi}_2\text{SrTa}_2\text{O}_9$  along (a) [001] and (b) [010]. Corresponding ED patterns are given in the insets. In panel b, two simulated images for *P*- and *I*-type cells (middle) and an enlarged, simulated image (right) are also presented.

basis of a tetragonal cell, consistent with the XRD results. The HREM image exhibits a regular dot array, which is identical to [100] images of cubic perovskite oxides. The ED pattern along the [010] zone and the corresponding HREM image of the acid-treated product are shown in Figure 3b. The HREM image can be explained on the basis of a lamellar structure. These observations clearly indicate that the structure of the perovskite-like slabs is retained after the acid treatment. We emphasize that all the examined particles of the acid-treated product (several hundreds) were crystalline on the basis of the ED analysis.

A Bi:Sr:Ta metal composition ratio of 2.0:0.98:2.0 was found for  $\text{Bi}_2\text{SrTa}_2\text{O}_9$  by ICP, consistent with the nominally indicated ratio. The composition of metals was drastically changed to 0.19:0.79:2.0 after the acid treatment. Taking the ED and HREM results into account, we ascribe the loss of the large portion of bismuth to the selective leaching of the bismuth oxide sheets in  $\text{Bi}_2\text{SrTa}_2\text{O}_9$ . The remaining bismuth (Bi:Ta = 0.19:2) and the loss of a corresponding amount of strontium (Sr:Ta = 0.19:2) should be ascribed to cation disorder ( $\text{B} \leftrightarrow \text{Sr}$ ), which was observed in our previous study on  $\text{Bi}_2\text{SrNaNb}_3\text{O}_{12}$ <sup>10</sup> and structural analyses of other Aurivillius phases.<sup>17,18</sup> Hence, the composition of the perovskite-like slabs in  $\text{Bi}_2\text{SrTa}_2\text{O}_9$  and its acid-treated product should be  $\text{Sr}_{0.8}\text{Bi}_{0.2}\text{Ta}_2\text{O}_7$ .

The amount of hydrogen in the acid-treated product was determined by TG (Figure 4). The acid-treated product heated at 120 °C exhibits a mass loss (2.7 wt %) starting at ~180 °C. The mass loss, ascribed to dehydration, corresponds to 1.8 H

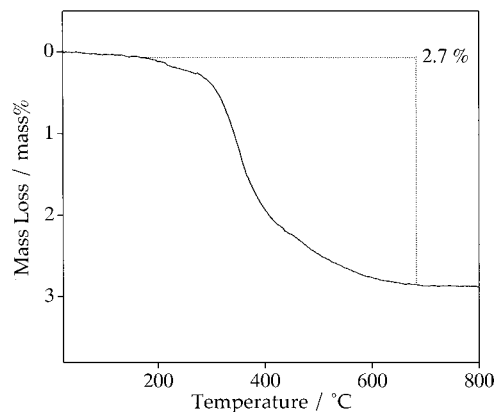
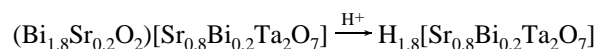


**Figure 4.** TG curve of acid-treated  $\text{Bi}_2\text{SrTa}_2\text{O}_9$  heated at 120 °C.

per  $\text{Sr}_{0.8}\text{Bi}_{0.2}\text{Ta}_2\text{O}_7$ . Since the layer charge of the perovskite-like slab is  $-1.8$  due to cation disorder ( $[\text{Sr}_{0.8}\text{Bi}_{0.2}\text{Ta}_2\text{O}_7]^{1.8-}$ ), the amount of hydrogen is in good agreement with the following overall reaction:



Suzuki et al.<sup>13</sup> reported the acid treatment of a  $\text{Bi}_2\text{SrTa}_2\text{O}_9$  single crystal. In the XRD pattern of the acid-treated  $\text{Bi}_2\text{SrTa}_2\text{O}_9$ , a series of peaks assignable to a  $00l$  reflection was observed, and the position of the low-angle peak ( $d = 0.9807$  nm) is close to the  $c$  parameter in the present study. Thus, the reported structural change of the  $\text{Bi}_2\text{SrTa}_2\text{O}_9$  single crystal appears to be identical to that observed in the present reaction.

**Structure of  $\text{H}_{1.8}[\text{Sr}_{0.8}\text{Bi}_{0.2}\text{Ta}_2\text{O}_7]$ .** Stacking sequences of the perovskite-like slabs in the layered perovskites depend on both compositions of the perovskite-like slabs and interlayer cations.<sup>19,20</sup> In a simple stacking sequence, an adjacent perovskite-like slab is located exactly above the other perovskite-like slab without displacement. It is also possible that an adjacent perovskite-like slab is stacked with displacement. For protonated forms of the layered perovskites, two types of stacking sequences of the perovskite-like slabs were reported: the simple stacking sequence without displacement<sup>2,6,8,19,21,22</sup> and the stacking sequence with a displacement by  $(a + b)/2$ .<sup>4,9a,23,24</sup> The unit cells of protonated phases possessing the simple stacking sequences contain only one perovskite-like slab, and the space group reported so far is  $P4/m$  for  $\text{H}[\text{LaNb}_2\text{O}_7]$ .<sup>19</sup> On the contrary, the relative displacement by  $(a + b)/2$  leads to a doubling of  $c$  parameters, and the structures of  $\text{H}_2[\text{SrNb}_2\text{O}_7]$  and  $\text{H}_2[\text{SrTa}_2\text{O}_7]$  (heated at 300 °C) were reported to possess *I*-type tetragonal cells.<sup>9a</sup> These previous reports suggest that either a unit cell with a simple stacking of the perovskite-like slabs (most likely a tetragonal *P*-type cell) or a unit cell with a stacking of the perovskite-like slabs with a displacement by  $(a + b)/2$  (a tetragonal *I*-type cell) appears to be adopted for  $\text{H}_{1.8}[\text{Sr}_{0.8}\text{Bi}_{0.2}\text{Ta}_2\text{O}_7]$ . The presence of the (100) peak in both the XRD and ED patterns (the (100) peak does not appear for tetragonal *I*-type

(19) Sato, M.; Abo, J.; Jin, T.; Ohta, M. *J. Alloys Compd.* **1993**, *192*, 81.

(20) Toda, K.; Teranishi, T.; Ye, Z.-G.; Sato, M.; Hinatsu, Y. *Mater. Res. Bull.* **1999**, *34*, 971.

(21) Gopalakrishnan, J.; Bhat, V.; Raveau, B. *Mater. Res. Bull.* **1987**, *22*, 413.

(22) Palacín, M. R.; Lira, M.; García, J. L.; Caldés, M. T.; Casañ-Pastor, N.; Fuertes, A.; Gómez-Romero, P. *Mater. Res. Bull.* **1996**, *31*, 217.

(23) Richard, M.; Brohan, L.; Tournoux, M. *J. Solid State Chem.* **1994**, *112*, 345.

(24) Schaak, R. E.; Mallouk, T. E. *J. Solid State Chem.* **2000**, *155*, 46–54.

(17) Blake, S. M.; Falconer, M. J.; McCreedy, M.; Lightfoot, P. *J. Mater. Chem.* **1997**, *7*, 1609.

(18) Ismunandar; Kennedy, B. J. *J. Mater. Chem.* **1999**, *9*, 541.

cells) and the lack of doubling of the  $c$  parameter ( $0.98 \pm 0.01$  nm) suggest that the structure of  $\text{H}_{1.8}[\text{Sr}_{0.8}\text{Bi}_{0.2}\text{Ta}_2\text{O}_7]$  possesses a  $P$ -type cell as an average structure.

Closer inspection of the structure of  $\text{H}_{1.8}[\text{Sr}_{0.8}\text{Bi}_{0.2}\text{Ta}_2\text{O}_7]$  by HREM provides further information on the stacking sequence. The HREM image along the [010] shows the presence of two types of stacking sequences (Figure 3b). To interpret this image, we simulated HREM images of  $\text{H}_{1.8}[\text{Sr}_{0.8}\text{Bi}_{0.2}\text{Ta}_2\text{O}_7]$  for both  $P$ -type (no displacement) and  $I$ -type (relative displacement by  $(a + b)/2$ ) cells. In simulated images, black dots are assigned to  $\text{TaO}_6$  octahedrons, and the displacement in the  $I$ -type cell is clearly demonstrated. The comparison of these two images with an enlarged image of  $\text{H}_{1.8}[\text{Sr}_{0.8}\text{Bi}_{0.2}\text{Ta}_2\text{O}_7]$  indicates that the two observed types of stacking sequences correspond to  $P$ - and  $I$ -type cells. Obvious streaks along  $c^*$  in the corresponding ED pattern (taken with the [010] incidence) are consistent with this stacking disorder.

### Conclusions

$\text{Bi}_2\text{SrTa}_2\text{O}_9$  was converted into  $\text{H}_{1.8}[\text{Sr}_{0.8}\text{Bi}_{0.2}\text{Ta}_2\text{O}_7]$  via acid treatment. HREM observations and diffraction results (XRD and ED) of  $\text{H}_{1.8}[\text{Sr}_{0.8}\text{Bi}_{0.2}\text{Ta}_2\text{O}_7]$  clearly revealed that  $\text{H}_{1.8}[\text{Sr}_{0.8}\text{Bi}_{0.2}\text{Ta}_2\text{O}_7]$  retained the structure of the perovskite-

like slabs in  $\text{Bi}_2\text{SrTa}_2\text{O}_9$ . Since no morphological change occurred during the acid treatment, the conversion reaction proceeded via the selective leaching of the bismuth oxide sheets in  $\text{Bi}_2\text{SrTa}_2\text{O}_9$ . HREM observations further demonstrated that two types of stacking sequences ( $P$ - and  $I$ -type) were present in  $\text{H}_{1.8}[\text{Sr}_{0.8}\text{Bi}_{0.2}\text{Ta}_2\text{O}_7]$ . The present reaction is the second successful conversion of the Aurivillius phase into the protonated form of the layered perovskite, and the present results strongly suggest that this type of conversion reaction can be applicable to various Aurivillius phases. Very recently, the conversion of a Ruddlesden–Popper phase ( $\text{K}_2[\text{La}_2\text{Ti}_3\text{O}_{10}]$ ) into an Aurivillius phase ( $\text{Bi}_2\text{La}_2\text{Ti}_3\text{O}_{12}$ ) was reported and corresponds to the reverse reaction of our conversions.<sup>25</sup> Hence, the Ruddlesden–Popper phases and the Aurivillius phases are likely to be interconvertible using newly discovered reactions.

**Acknowledgment.** This work was financially supported in part by a Grant-in-Aid for Scientific Research (Grant 10555221) from the Ministry of Education, Science, Sports, and Culture of Japan.

IC010266M

(25) Gopalakrishnan, J.; Sivakumar, T.; Ramesha, K.; Thangadurai, V.; Subbanna, G. N. *J. Am. Chem. Soc.* **2000**, *122*, 6237.